Air-stable Fe and Co crystalline nanocomposite particles prepared by a single-step swelling of metal precursors within polystyrene microspheres of narrow size distribution

Nava Shpaisman and Shlomo Margel*

Received (in Gainesville, FL, US) 5th February 2007, Accepted 25th April 2007
First published as an Advance Article on the web 18th May 2007
DOI: 10.1039/b701730h

Polystyrene template microspheres of narrow size distribution were prepared by dispersion polymerization of styrene in a mixture of ethanol and 2-methoxyethanol. These template particles, dispersed in an aqueous solution, have been used to entrap $Fe_3(CO)_{12}$ and $Co_2(CO)_8$ complexes, using a single-step swelling process of methylene chloride and benzene emulsion droplets containing these complexes, within the particles. The effect of the swelling solvents (methylene chloride and benzene) on the size and size distribution of the swollen template particles was elucidated. Air-stable Fe and Co nanocomposite particles have been prepared by thermal decomposition of the $Fe_3(CO)_{12}$ and $Co_2(CO)_8$ swollen template particles at 600 °C in an inert atmosphere. These nanocomposite particles have a core-shell structure, where a thin coating of metal oxide and carbon protects the core crystalline metal (Fe and Co) from oxidation. The characterization of the various microspheres and the air-stable Fe and Co nanocomposite particles was accomplished by light microscopy, TEM, SEM, XRD, XPS, elemental analysis, and magnetic measurements.

Introduction

The synthesis of magnetic nanoparticles is of interest to researchers in both academia and industry due to its wide range of application in magnetic and electronic devices,[1–3] medicine,[4] and new technologies such as environmental remediation.[5] The magnetic behavior of these systems has been found to be particularly dependent on their crystalline character and on their size and size distribution. Co and Fe nanoparticles are of special interest since these metals have the highest magnetic moments among the ferromagnetic transition metals. However, Fe and Co nanoparticles are easily oxidized, *e.g.* by air, and thereby significantly lose their main advantage of a very high magnetic moment. Intensive efforts have been made toward coating and protecting Fe and Co nanoparticles from air oxidation. Air-stable Fe or Co particles have been prepared by different methods, *e.g.* embedding the particles in polymer matrices,[6,7] passivating them with an oxide shell,[2] carbonizing Fe powder with methane, thereby producing iron carbide embedded in a carbon matrix,[7–10] and high temperature annealing of mixtures of hematite and carbon powders.[1] The present article describes a simple process to prepare air-stable Fe and Co nanocomposite particles, based on a single-step swelling of polystyrene (PS) template microspheres with $Fe_3(CO)_{12}$ or $Co_2(CO)_8$, followed by the thermal decomposition of the template particles containing these metal complexes in an inert atmosphere.

Department of Chemistry, Bar-Ilan University, Ramat-Gan 52900, Israel. E-mail: shlomo.margel@mail.biu.ac.il. E-mail: ch152@mail.biu.ac.il; Fax: +972-3-5351250; Tel: +972-3-5318725

Ugelstad and co-workers invented a useful, multi-step swelling method of uniform template particles with various acrylate monomers and initiators, for the production of different uniformly-sized particles with controllable properties.[11,12] The first step of the multi-step swelling method is associated with the activation of uniform template particles (usually PS). The activation of these particles is accomplished by swelling the particles dispersed in an aqueous phase with emulsion droplets of a swelling solvent, *e.g.* dibutyl phthalate, methylene chloride, toluene, or 1-chlorodecane. The first swelling step stimulates the swelling of the template particles in the subsequent steps. When the activation swelling step is completed, the second swelling step takes place by introducing the slightly enlarged template particles to monomers, initiator and porogens. This can be done in one step, or through the sequential addition of each component. The polymerization of the monomers within the uniformly-swollen particles can then be induced by increasing the temperature. An alternative swelling method, called "the dynamic swelling method",[13] was invented by Okubo *et al.* According to this method, uniform PS template particles can be swollen significantly, while maintaining their uniformity, by the slow, continuous, dropwise addition of water into an ethanol–water medium containing the template particles and the hydrophobic monomer(s) and initiator (*e.g.* styrene and benzoyl peroxide). Polymerization can then be performed, as previously described, by increasing the temperature. According to the dynamic swelling method, there is no need to use a swelling solvent, and the process can be performed in a one-step procedure. A new method for preparing particles of narrow size distribution and controlled chemical properties, based on a single-step swelling process of template uniform microspheres, was recently published by

Margel *et al.*[14,15] According to this process, the swelling of the template particles with the initiator and monomer(s) *via* a swelling solvent is accomplished in a single step, in contrast to the multi-swelling steps where the swelling with these reagents is accomplished in two or more sequential steps. Recently, we used the single-step swelling process to entrap $Fe(CO)_5$ rather than acrylate monomers within the PS template microspheres. The $Fe(CO)_5$ swollen particles were then used for the formation of air-stable Fe nanocrystalline particles by the thermal decomposition of the swollen template particles at 600 °C in an inert atmosphere.[16] However, $Fe(CO)_5$ is highly toxic.[17] In addition, the yield of the entrapped Fe within the nanocomposite particles is low. $Fe(CO)_5$ evaporates at 103 °C, so a substantial part of the entrapped complex evaporates before the decomposition of the PS at 600 °C. The present manuscript describes a method to prepare air-stable Fe and Co nanocomposite particles by a similar single-step swelling process, substituting $Fe(CO)_5$ for $Fe_3(CO)_{12}$ or $Co_2(CO)_8$. $Fe_3(CO)_{12}$ is two thousand times less toxic than $Fe(CO)_5$.[17] Furthermore, $Fe_3(CO)_{12}$ and $Co_2(CO)_8$ are solid powders that decompose to the relevant metals at 150 °C and 90 °C, respectively, without melting, while $Fe(CO)_5$ evaporates at 103 °C and decomposes at 380 °C.[18]

Experimental

Materials

The following analytical-grade chemicals were purchased from Aldrich, and were used without further purification: $Fe_3(CO)_{12}$ powder protected by 5–10% w/w methanol, $Co_2(CO)_8$ powder protected by 10% w/w hexane, benzoyl peroxide (BP) 98%, sodium dodecyl sulfate (SDS), polyvinylpyrrolidone (PVP, MW 360 000), ethanol (HPLC), 2-methoxyethanol (HPLC), benzene (HPLC), and methylene chloride (HPLC). Styrene (Aldrich 99%) was passed through activated alumina (ICN) to remove inhibitors before use. Water was purified by passing de-ionized water through an Elgastat Spectrum reverse osmosis system (Elga Ltd, High Wycombe, UK).

Synthesis of polystyrene template microspheres

Uniform PS template microspheres, of 2.7 ± 0.3 μm diameter, coated with PVP, were prepared by dispersion polymerization of styrene in a mixture of ethanol and 2-methoxyethanol in the presence of the stabilizer PVP, according to the literature.[16,19,20]

Single-step swelling of polystyrene template microspheres with $Fe_3(CO)_{12}$ and $Co_2(CO)_8$

PS template microspheres of 2.7 ± 0.3 μm diameter, were swollen with methylene chloride containing $Fe_3(CO)_{12}$, or benzene containing $Co_2(CO)_8$, according to the following procedure: 2 ml of methylene chloride containing 5% $Fe_3(CO)_{12}$ were added to a 20 ml vial containing 10 ml of a 1.5% (w/v) SDS aqueous solution. Emulsion droplets of the methylene chloride solution were then formed by sonication (Sonics and Materials, model VCX-750, Ti-horn 20 KHz) of the former mixture at 4 °C for 30 s. 3.5 ml of an aqueous suspension of the PS template microspheres (7% w/v) were then added to the stirred emulsion. After the swelling was completed, and the mixture did not contain any small emulsion droplets of methylene chloride containing $Fe_3(CO)_{12}$, as verified by optical microscopy, the diameter of the swollen microspheres was measured. Evaporation of the entrapped methylene chloride was then performed by mild purging with nitrogen at room temperature for *ca.* 4 h through the shaken, open vial containing the swollen particle aqueous mixture. The excess reagents were then washed from the PS particles containing the entrapped $Fe_3(CO)_{12}$ by several centrifugation cycles with water, and the particles then dried under a nitrogen flow for a few hours. A similar process, substituting the 2 ml methylene chloride containing 5% $Fe_3(CO)_{12}$ for benzene containing 5% $Co_2(CO)_8$, was performed for entrapping the cobalt complex within the PS template microspheres.

Synthesis of air-stable Fe and Co nanocomposite particles

Air-stable Fe and Co nanocomposite particles were formed by heating the dried PS particles containing the entrapped metal complexes in a quartz tube at 600 °C under flowing Ar gas for 3 h.

Characterization of the particles

Optical microscope pictures were obtained with an Olympus microscope, model BX51. The microspheres' average size and size distribution were determined by measuring the diameters of more than 100 particles on optical micrographs with image analysis software, AnalySIS Auto (Soft Imaging System GmbH, Germany). Surface morphology was characterized with a JEOL scanning electron microscope (SEM) (model JSM-840). Low resolution, transmission electron microscope (TEM) pictures were obtained with a JEOL-JEM100SX electron microscope with a 80–100 kV accelerating voltage. High-resolution TEM (HRTEM) images were obtained by employing a JEOL-3010 device with a 300 kV accelerating voltage. Samples for TEM and HRTEM were prepared by placing a drop of the diluted sample on a 400-mesh carbon-coated copper grid. Fourier transform infrared (FTIR) analysis was performed with a Bomem FTIR spectrophotometer, model MB100, Hartmann & Braun. The analysis was performed with 13 mm KBr pellets that contained 2 mg of the detected material and 198 mg KBr. The pellets were scanned over 200 scans at a 4 cm^{-1} resolution. Elemental analysis of the various nanocomposite particles was performed using an elemental analysis instrument, model EA1110, CE Instruments, Thermoquast. Surface elemental analysis was obtained by X-ray photoelectron spectroscopy (XPS), model AXIS-HS, Kratos Analytical, England, using Al Kα lines, at 10^{-9} Torr, with a take-off angle of 90°. The reported values of both the XPS and the elemental analysis are an average of measurements performed on at least three samples of each of the tested particles, and have a maximum error of about 10 and 2%, respectively. Powder X-ray diffraction (XRD) patterns were recorded using an X-ray diffractometer (model D8 Advance, Bruker AXS) with Cu Kα radiation. Magnetic measurements were performed on a sample that was introduced into a plastic capsule. Measurements at room temperature were performed using an Oxford Instrument vibrating sample magnetometer (VSM).

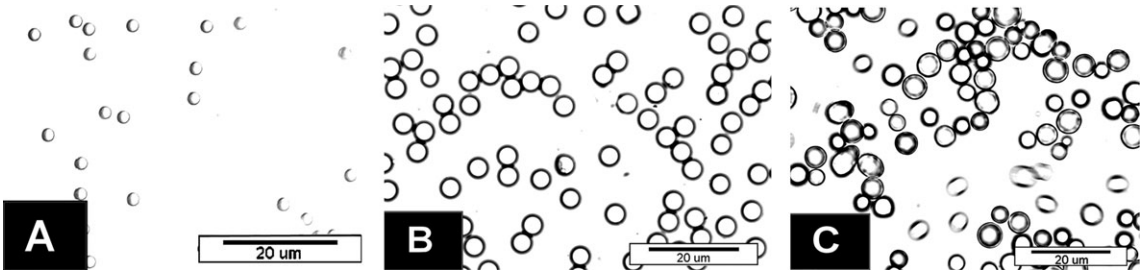

Fig. 1 Light microscope pictures of PS template microspheres (A), and PS template microspheres swollen with 2 ml methylene chloride containing 100 mg of $Fe_3(CO)_{12}$ (B), or 2 ml benzene containing 100 mg of $Co_2(CO)_8$ (C). The swelling process was accomplished according to the experimental section.

Magnetization was measured as a function of the external field being swept up and down ($-16\,000$ Oe $< H_{applied} <$ 16 000 Oe, in steps of 200 Oe).

Results and discussion

The swelling of the PS template microspheres was accomplished with two swelling solvents, methylene chloride and benzene, both of which are known to be efficient swelling solvents for PS microspheres.[8,21] Methylene chloride is a good solvent for $Fe_3(CO)_{12}$, but scarcely dissolved the $Co_2(CO)_8$. On the other hand, benzene is quite a good solvent for $Co_2(CO)_8$, but not for $Fe_3(CO)_{12}$. Fig. 1A–C show light microscope pictures that allow one to compare the swelling ability of the PS template particles by methylene chloride and benzene containing 5% (w/v) $Fe_3(CO)_{12}$ or $Co_2(CO)_8$, respectively. Before swelling, the PS template microspheres had a size and size distribution of 2.7 ± 0.3 μm (Fig. 1A). As a consequence of their swelling with 2 ml of methylene chloride containing $Fe_3(CO)_{12}$, their size distribution was retained, while their diameter increased to 4.8 ± 0.3 μm, *ca.* a 220% increase in the average diameter (Fig. 1B). On the other hand, a similar swelling process, substituting the methylene chloride containing the Fe complex for benzene containing the Co complex, resulted in an increased size and size distribution from 2.7 ± 0.3 μm to 6.2 ± 1.2 μm, *ca.* a 300% increase in the average diameter, and a significant increase in the size distribution. It should be noted that the swelling behavior of the PS template particles by methylene chloride or benzene in the absence or presence of 5% of the metal complexes was similar. This behavior indicates that the main contributors to the swelling of the PS template particles are methylene chloride and benzene, while the contributions of $Fe_3(CO)_{12}$ and $Co_2(CO)_8$ to the swelling are negligible. It should also be noted that addition of 5 ml, instead of 2 ml, methylene chloride or benzene resulted in total dissolution of the PS template particles. The completion of the swelling process was verified by optical microscopy, as indicated in the experimental section, by the disappearance of the small droplets of the emulsified methylene chloride or benzene from the swollen particle mixture, indicating that all the metal complexes are either entrapped within the PS particles or adsorbed on their surfaces.

After completion of the swelling process, the swelling solvents were removed from the particles by mild purging with nitrogen at room temperature for *ca.* 4 h through the shaken, open vial containing the swollen particle aqueous mixture. The evaporation of the swelling solvents leads to the contraction of the particles containing the Fe and Co complexes from 4.8 ± 0.3 to 2.9 ± 0.3 μm and from 6.2 ± 1.2 to 2.7 ± 0.4 μm, respectively. Fig. 2 illustrates with SEM pictures the smooth surface of the PS microspheres (A), in contrast to the rougher surfaces of the PS microspheres containing the metal complexes (B & C). This surface roughness may be due to adsorption of the metal complexes on the particles' surfaces. Fig. 2C illustrates that the surface roughness of microspheres containing the Co complex is significantly higher than that of those containing the Fe complex (Fig. 2B). This difference may indicate that the Co complex is adsorbed on the surface of the PS particles to a much higher extent than the Fe complex. Indeed, XPS surface analysis of the particles containing the metal complexes illustrated that the surface concentration of Fe is 2.4 times lower than that of Co: 2.4 and 7.0%, respectively.

Fig. 3 depicts the FTIR spectra of the PS template microspheres (A), $Fe_3(CO)_{12}$ (B), $Co_2(CO)_8$ (C), and PS template

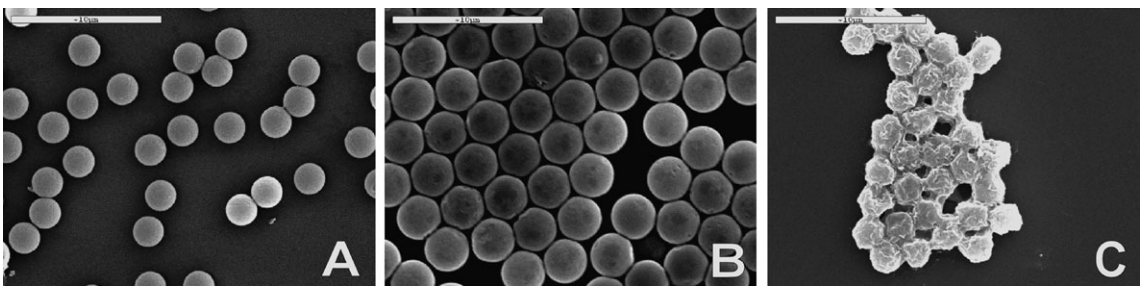

Fig. 2 SEM pictures of the PS template microspheres (A) and the PS microspheres containing $Fe_3(CO)_{12}$ (B) or $Co_2(CO)_8$ (C). The swelling process and the evaporation of the swelling solvents were accomplished according to the experimental section.

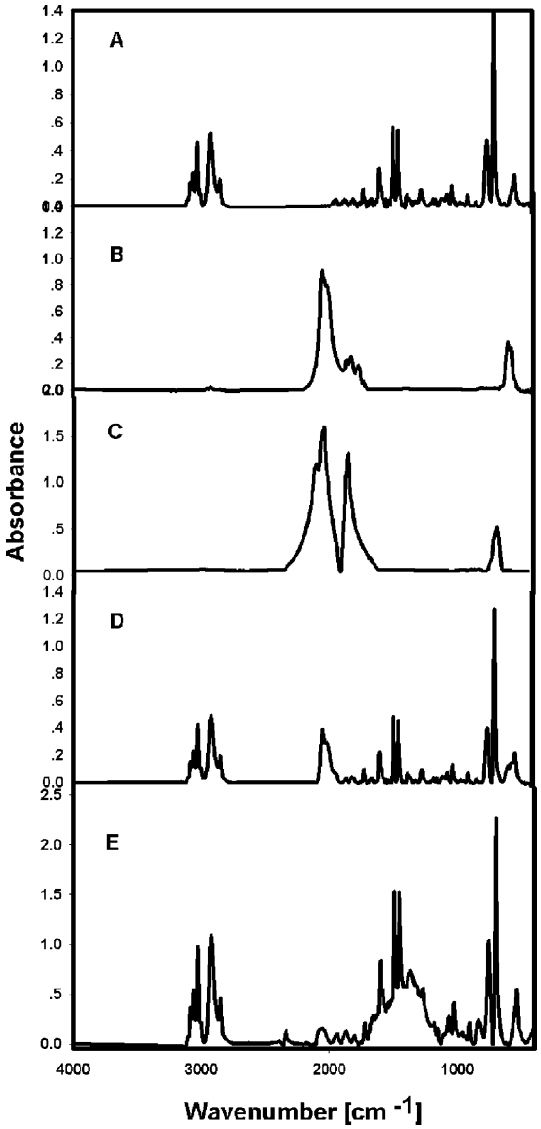

Fig. 3 FTIR spectra of the PS template microspheres (A), $Fe_3(CO)_{12}$ (B), $Co_2(CO)_8$ (C), and the PS template microspheres containing $Fe_3(CO)_{12}$ (D) or $Co_2(CO)_8$ (E). The PS microspheres containing the $Fe_3(CO)_{12}$ or $Co_2(CO)_8$ were prepared according to the experimental section.

particles containing $Fe_3(CO)_{12}$ (D) or $Co_2(CO)_8$ (E). Fig. 3A reveals a typical IR spectrum of PS: the peaks at 1492 and 3000–3100 cm^{-1} correspond to the aromatic CH stretching bands, 2849 and 2922 cm^{-1} to the CH_2 stretching bands and 700 cm^{-1} to the C–C vibration band. Fig. 3B reveals an IR spectrum of $Fe_3(CO)_{12}$: 1900–2100 cm^{-1} corresponds to the CO stretching bands (the terminal M–CO and the doubly-bridging CO) and 555 cm^{-1} to the Fe–C stretching band. Fig. 3C reveals an IR spectrum of $Co_2(CO)_8$: 2100 cm^{-1} corresponds to the terminal M–CO stretching band, 1850 cm^{-1} to the doubly-bridging CO stretching band and 570 cm^{-1} to the Co–C stretching band. Fig. 3D demonstrates the presence of $Fe_3(CO)_{12}$ in the PS microspheres, by illustrating peaks belonging both to PS (700, 1492, 3000 cm^{-1}, *etc.*) and to $Fe_3(CO)_{12}$ (2100 cm^{-1}, 550 cm^{-1}, *etc.*). Surprisingly, the spectrum shown in Fig. 3E does not fit that expected for the PS microspheres containing the Co complex, since the peaks belonging to the complex do not match those of $Co_2(CO)_8$. This result is difficult to understand and requires further investigation. We assume that the peaks at *ca.* 1550 cm^{-1} belong to $Co_7(CO)_{15}$, which, produced from the $Co_2(CO)_8$, is entrapped within the PS particles, as reported in the literature.[22]

Table 1 XPS surface elemental analysis of the Fe and Co nanocomposite particles

	Surface elemental analysis (wt%)		
Nanocomposite type	C	O	Metal
Fe	74	21.7	4.3
Co	79.4	17.7	2.9

Air-stable Fe and Co nanocomposite particles were formed by heating the dried PS particles containing the $Fe_3(CO)_{12}$ or $Co_2(CO)_8$ in a quartz tube at 600 °C under Ar atmosphere, according to the experimental section. Tables 1 and 2 illustrate the surface and bulk composition of the Fe and Co nanocomposite particles, as studied by XPS[23,24] and elemental analysis, respectively.

These tables show that the surface concentration of C and O is significantly higher than that of the bulk, *e.g.*, the surface and bulk concentrations of C in the Fe nanocomposite particles are 74 and 17.8%, respectively. The higher concentration of O on the surface is probably due to the surface oxidation of Fe and carbon. On the other hand, the surface concentrations of Fe (4.3%) and Co (2.9%) of these nanocomposite particles are significantly lower than those of the bulk (69.8 and 71.8%, respectively). These results may indicate that the core of these nanocomposite particles is mainly composed of metals coated by a shell of carbon and metal oxides.

In previous work,[16] Fe nanocomposite particles were prepared similarly, substituting the trapping of 0.2 mmol $Fe_3(CO)_{12}$ within the PS template microspheres for 7.0 mmol $Fe(CO)_5$. However, in spite of the significantly higher concentration of $Fe(CO)_5$ [7.0 mmol] compared to $Fe_3(CO)_{12}$ [0.2 mmol], the yield of trapped Fe in the nanocomposite particles formed with $Fe(CO)_5$ was lower: 47 and 69.8%, respectively. The lower yield of trapped Fe within the nanocomposite particles on using $Fe(CO)_5$ as the Fe source may be explained by the low boiling temperature of this complex (bp 103 °C, decomposition temperature 380 °C), so that a substantial part of the entrapped complex evaporates before the decomposition of the PS at 600 °C. On the other hand, $Fe_3(CO)_{12}$ and $Co_2(CO)_8$ are solid powders that decompose to the relevant metals at 150 °C and 90 °C, respectively, without melting.[18]

Table 2 Elemental analysis of the Fe and Co nanocomposite particles

	Elemental analysis (wt%)			
Nanocomposite type	C	H	O	Metal[a]
Fe	17.8	0.6	11.8	69.8
Co	18.8	0.5	8.9	71.8

[a] The Fe and Co nanocomposite particles were prepared according to the experimental section. The % Fe and Co was calculated by reducing from 100 the % of the sum of the other elements (C, H, and O).

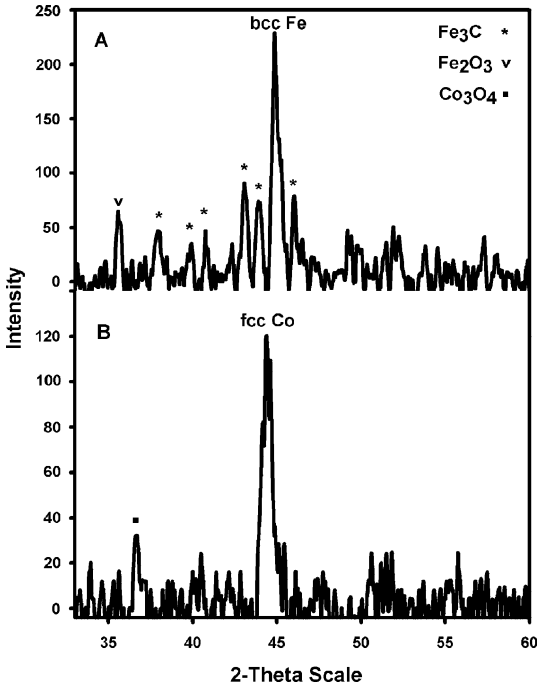

Fig. 4 XRD patterns of the Fe (A) and Co (B) nanocomposite particles. The Fe and Co nanocomposite particles were prepared according to the experimental section.

Fig. 4A and B show the XRD patterns of the Fe and Co nanocomposite particles decomposed at 600 °C for 3 h under argon atmosphere. The XRD data of the Fe nanocomposite particles (Fig. 4A) reveal the presence of body-centered cubic (bcc)-Fe at $2\theta = 44.8°$, cementite Fe_3C at $2\theta = 38$, 42.3, 40.8, 44, 44.9, 46°, and Fe_3O_4 at $2\theta = 35.6°$. The XRD spectrum of the Co nanocomposite particles (Fig. 4B) consists of fcc-Co at $2\theta = 44.4°$, and a small amount of Co_3O_4 at $2\theta = 36.6°$.

The magnetization curves presented in Fig. 5 show well-defined hysteresis loops of the Fe (A) and Co (B) nanocomposite particles, which exhibit ferromagnetic behavior. The $M(H)$ plots of both metal nanocomposite particles reach saturation in fields around 5000 Oe. The saturation magnetization (M_S), remanent magnetization (M_R), and coercivity

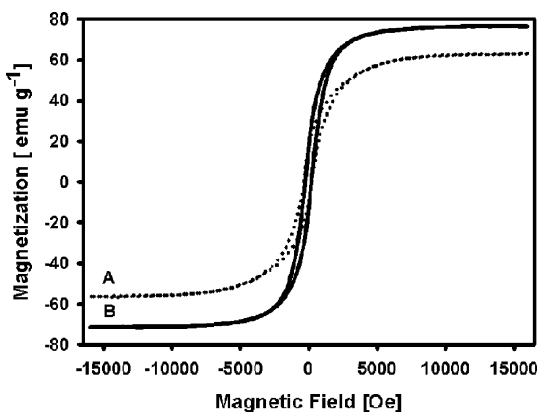

Fig. 5 Magnetization curves of the Fe (A) and Co (B) nanocomposite particles. The Fe and Co nanocomposite particles were prepared according to the experimental section.

Table 3 Magnetic properties of the Fe and Co nanocomposite particles

Nanocomposite type	M_S/emu g^{-1}	M_R/emu g^{-1}	H_C/Oe
Fe	63	16	295
Co	76.6	18	247

(H_C) of the Fe and Co nanocomposite particles, are illustrated in Table 3. The saturation magnetization and coercivity of the Fe nanocomposite particle are 63 emu g^{-1} and 295 Oe, respectively. The reported values of bulk bcc-Fe are 222 emu g^{-1} and 40 Oe.[25] The lower M_S and the higher H_C can be explained by the composition of these nanocomposite particles: approximately 70% Fe, and 30% C, O and H (see Table 2). Furthermore, the Fe nanocomposite particles contain, in addition to bcc-Fe, a substantial concentration of Fe_3C and Fe_3O_4 (see Fig. 4), and the M_S values of Fe_3C (14 emu g^{-1}) and Fe_3O_4 (75 emu g^{-1}) are significantly lower than that of bcc-Fe (222 emu g^{-1}).[26,27] The H_C value of Fe_3C is also higher than that of bcc-Fe.[27]

Table 3 also illustrates that the M_S of the Co nanocomposite particles is 77 emu g^{-1}, significantly lower than that of crystalline fcc-Co (M_S = 160 emu g^{-1}).[28] As previously stated, this difference can be explained by the composition of the Co nanocomposite particles (approximately 70% Co and 30% C, H and O), and the substantial presence of Co_3O_4 in the nanocomposite particles, which possess M_S of 0.001 emu g^{-1}.[29] However, the presence of an oxide layer can be the cause for enhancing the resulting coercivity from a few tens to a few hundreds of Oe in the Co nanocomposite particles.[30–32]

The TEM images of the Fe and Co nanocomposite particles (Fig. 6A and B, respectively) illustrate monodispersed particles of an average diameter and size distribution of 210 ± 76 and 130 ± 60 nm, respectively. The size distribution of these nanocomposite particles is significantly superior to that of the Fe nanocomposite particles obtained by using $Fe(CO)_5$ as a precursor for Fe: 305 ± 110 nm.[16] HRTEM images of the Fe and Co nanocomposite particles (Fig. 6C and D) show that these particles have a core-shell structure wherein the shell thickness of both nanoparticles is approximately 5 nm. Fig. 6C demonstrates that the coating of the Fe particles is composed of internal and external layers with *d*-spacings of 2.56 and 3.32 Å, respectively. These interlayer distances may indicate that the internal one is composed of Fe_3O_4 and the external one of graphite.[25] The electron diffraction patterns of the Fe and Co nanocomposite particles (Fig. 6E and F) show the distinct patterns of the crystalline composites. The intensities of the diffraction ring/spots shown in Fig. 6E are 2.08 and 1.47 Å, consistent with metallic iron (bcc-Fe: 2.03, 1.43 Å), and 2.57 Å, which corresponds to Fe_3O_4.[33] The intensities of the diffraction spots shown in Fig. 6F are 2.06, 1.83 and 1.3 Å that match fcc-Co, while 2.45 and 4.7 Å match Co_3O_4.

The storage stability at room temperature in air of the Fe and Co nanocomposite particles was tested by sequential XPS, elemental analysis, XRD, and magnetic susceptibility measurements. These measurements did not indicate any significant changes during one year's storage. Also, no visible change was observed during this period of time. The nanocomposite particles were also stable for at least one week upon contact

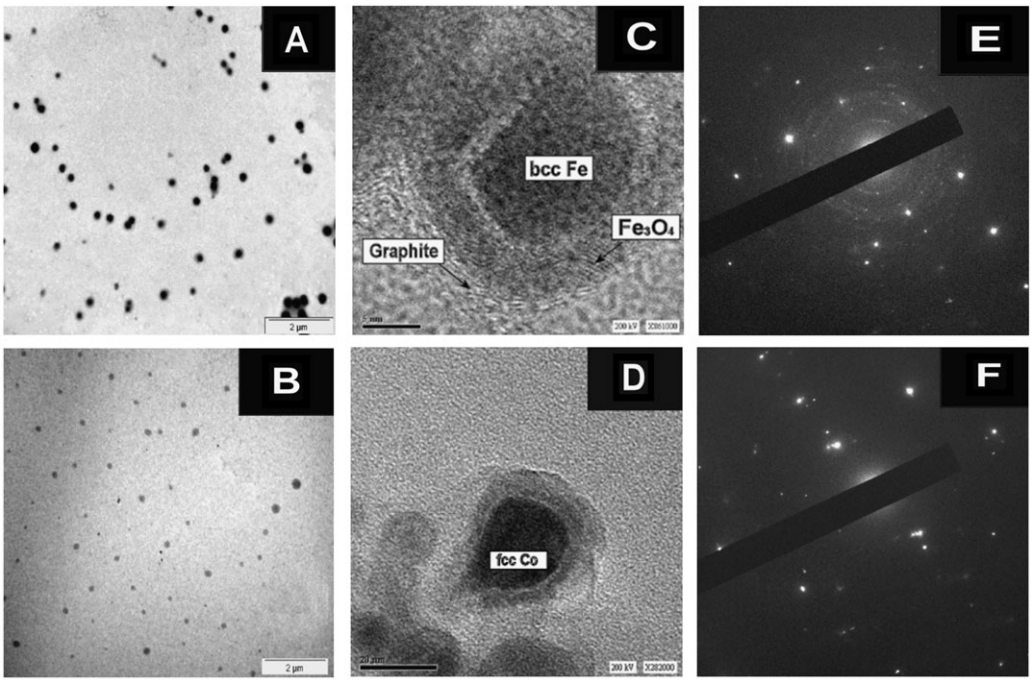

Fig. 6 Low resolution TEM pictures (A and B), HRTEM pictures (C and D), and electron diffraction patterns (E and F) of the Fe and Co nanocomposite particles, respectively. The Fe and Co nanocomposite particles were prepared according to the experimental section.

with water, 1 M aqueous NaOH solution, and ethanol. Treatment with 1 M HCl causes a rapid dissolution of the nanocomposite particles. The air-stability of these particles is probably due to the protective shell of carbon and Fe_3O_4 or Co_3O_4 around the metal cores.

Conclusions and future plans

This article describes a simple and efficient process for the synthesis of air-stable Fe and Co crystalline magnetic nanocomposite particles. The first step consists of encapsulation of the $Fe_3(CO)_{12}$ or $Co_2(CO)_8$ complexes within uniform PS template microspheres, by a single-step swelling process. Decomposition of the as-prepared PS particles containing the metal complexes at 600 °C under an argon atmosphere leads to the formation of air-stable Fe and Co nanocomposite particles. These nanoparticles are composed of a metal core coated by a carbon and metal oxide protective shell. This process for preparing the metal-containing nanocomposite particles is significantly superior to the former process reported by us,[16] through which air-stable Fe nanocomposite particles were prepared by a similar process, substituting the $Fe_3(CO)_{12}$ precursor for $Fe(CO)_5$. $Fe_3(CO)_{12}$ is two thousand times less toxic than $Fe(CO)_5$. The yield of Fe trapped within the nanocomposite particles using the $Fe_3(CO)_{12}$ precursor is significantly higher, and the monodispersity of the Fe nanocomposite particles observed in the present article is much superior to that obtained on using $Fe(CO)_5$ as the metal source. In future studies we wish to extend this approach for studies concerning PS template particles of lower diameters (*e.g.* below 1.0 μm), as well as for the preparation *via* a similar process of other air-stable magnetic nanocomposite particles, *e.g.* Ni.

Acknowledgements

We thank Prof. Yossi Yeshurun (Physics Dept, Bar-Ilan University, Israel) for his help with the magnetic measurements. Our study was partially supported by a Minerva Grant (Microscale & Nanoscale Particles and Films) and by The Israeli Ministry of Commerce and Industry (NFM Consortium on Nanocomposite Particles for Industrial Applications).

References

1 H. Toroko, S. Fujii and T. Oku, *Diamond Relat. Mater.*, 2004, **13**, 1270.
2 E. Shafranovsky and Y. Petrov, *J. Nanopart. Res.*, 2004, **6**, 71.
3 D. Harvey, R. Kalyanaraman and T. Sudarshan, *Mater. Sci. Technol.*, 2002, **18**, 959.
4 S. Rudge, C. Peterson, C. Vessely, J. Koda, S. Stevens and L. Catterall, *J. Controlled Release*, 2001, **74**, 335.
5 W. Zhang, *J. Nanopart. Res.*, 2003, **5**, 323.
6 J. Wilson, P. Poddar, N. Frey, H. Srikanth, K. Mohomed, J. Harmon, S. Kotha and J. Wachsmuth, *J. Appl. Phys.*, 2004, **95**, 1439.
7 V. F. Puntesa, K. Krishnanb and A. P. Alivisatosa, *Top. Catal.*, 2002, **19**, 145.
8 U. Narkiewcz, N. Guskos, W. Arabezik, J. Typek, T. Bodziony, G. Gaziorek, I. Kucharewcz and E. Anagnostakis, *Carbon*, 2004, **42**, 1127.
9 H. Huang, S. Yang and G. Gu, *J. Phys. Chem. B*, 1998, **102**, 3420.
10 A. Lu, W. Li, N. Matoussevitch, B. Spliethoff, H. Bönnemann and F. Schu, *Chem. Commun.*, 2005, 98.
11 J. Ugelstad, *Makromol. Chem.*, 1978, **179**, 815.
12 J. Ugelstad, P. C. Mork, I. Nordhuus, H. Mfutakamba and E. Soleimany, *Makromol. Chem. Suppl.*, 1985, **10–11**, 215.
13 M. Okubo, E. Ise and T. Yamashita, *J. Appl. Polym. Sci.*, 1999, **74**, 278.
14 L. Boguslavsky and S. Margel, *J. Polym. Sci., Part A: Polym. Chem.*, 2004, **42**, 4847.
15 U. Akiva and S. Margel, *J. Colloid Interface Sci.*, 2005, **288**, 61.
16 N. Shpaisman and S. Margel, *Chem. Mater.*, 2006, **18**(2), 396.

17 Threshold limit values (TLV) of iron pentacarbonyl and triiron dodecacarbonyl are 0.1 and 200 ppm, respectively, from the Material Safety Data Sheets (MSDS).
18 S. A. Mulenko and A. N. Pogorelyi, *J. Magn. Magn. Mater.*, 1996, **157–158**, 299.
19 V. Smigol and F. Svec, *J. Appl. Polym. Sci.*, 1992, **46**, 1439.
20 Y. C. Liang, F. Svec and J. M. Frechet, *J. Polym. Sci., Part A: Polym. Chem.*, 1997, **35**, 2631.
21 C. D. Sherrington, *Chem. Commun.*, 1998, 2275.
22 T. Funaioli, P. Biagini and G. Fachinetti, *Inorg. Chem.*, 1990, **29**, 1440.
23 H. Bamnolker and S. Margel, *J. Polym. Sci., Part A: Polym. Chem.*, 1996, **34**, 1857.
24 Q. S. Bhatia, D. H. Pan and J. T. Koberstein, *Macromolecules*, 1988, **21**, 2166.
25 S. I. Nikitenko, Y. Koltypin, O. Palchik, I. Felner, X. N. Xu and A. Gedanken, *Angew. Chem., Int. Ed.*, 2001, **40**, 4447.
26 D. Craik, *Magnetism: Principles and Applications*, Wiley, Toronto, 1995, p. 404.
27 P. S. Follansbee, *Metals Handbook*, American Society for Metals, Metal Park, OH, 9th edn, 1985, vol. 9, (Metallography and Microstructures).
28 M. J. Aus, C. Cheung, B. Szpunar, U. Erb and J. Szpunar, *J. Mater. Sci. Lett.*, 1998, **17**, 1949.
29 A. Quesada, M. A. García, M. Andrés and A. Hernando, *J. Appl. Phys.*, 2006, **100**, 113909.
30 S. Gangopadhyay, G. C. Hadjipanayis, B. Dale, C. M. Sorensen, K. J. Klabunde, V. Papaefthymiou and A. Kostikas, *Phys. Rev. B: Condens. Matter Mater. Phys.*, 1992, **45**, 9778.
31 A. Tsoukatos, H. Wan, G. C. Hadjipanayis, V. Papaefthymiou, A. Kostikas and A. Simopoulos, *J. Appl. Phys.*, 1993, **73**, 6967.
32 A. S. Edelstein, B. N. Das, R. L. Holtz, N. C. Koon, M. Rubinstein, S. A. Wolf and K. E. Kihlstrom, *J. Appl. Phys.*, 1987, **61**, 3320.
33 *Powder Diffraction File*, International Center for Diffraction Data, Swarthmore, PA, 1988, file # 6-696.